A COMPARISON OF MODE III AND MODE I TOUGHNESS IN QUENCHED AND TEMPERED STEELS

N. J. Hurd and P. E. Irving

GKN Technology Ltd., Birmingham New Road, Wolverhampton WV4 6BW, UK

ABSTRACT

Studies have been made of the fracture toughness in mode I and in mode III of low alloy steels quenched and tempered to a range of strength levels. It is found that the resistance to crack initiation decreases with increasing strength level in mode I whereas it increases with increasing strength level in mode III. The results are discussed in terms of the crack tip stress and strain fields operating in the two modes. Service failure modes in torsion are considered in the light of these results.

KEYWORDS

Torsional fracture; mode III; mode I; strength level; crack tip stress fields; crack tip strain fields; elastic plastic fracture.

INTRODUCTION

The mode III (antiplane strain) fracture configuration is generally considered to be theoretically useful, but of little practical significance (e.g. Sorensen, 1978). Frequent use has been made of the relative ease with which stress and strain distributions around the mode III crack tip can be obtained. Once such solutions were derived, their form was extended to the mode I case which is of more practical use (McClintock & Irwin, 1965; Rice, 1968).

In service, mode III fracture might be expected to occur predominantly in shafts loaded in torsion, where both transverse and longitudinal shear planes are found, (Fig. 1). In spite of this, there are many torsional failures which occur via mode I cracks at $\pm 45^{\circ}$ to the longitudinal axis of the shaft, along the plane of maximum principal tensile stress.

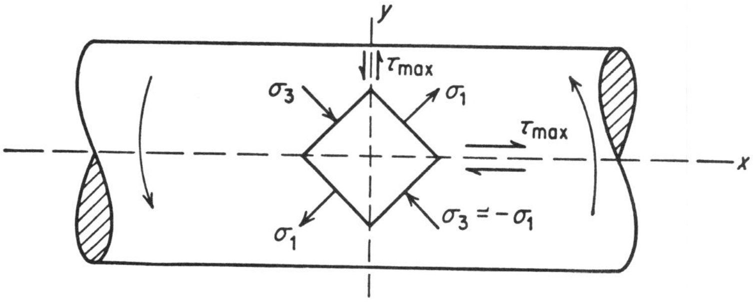

Fig. 1 Torsional stress state showing planes of shear and planes of principal tensile stress (Dieter, 1961)

However, production operations such as induction hardening are frequently used in an effort to improve the fatigue strength in torsion. The strength profile of the hardened shaft is then more nearly matched to the applied stress profile, and in addition there will be compressive residual stresses present. The latter have the effect of supressing mode I crack growth by reducing crack opening. Compressive residual stresses have little effect on the sliding modes of crack extension (Smith, 1980), and consequently torsional failures where compressive residual stresses are present tend to be dominated by cracks which have extended in modes II and III.

Examples of the sorts of failure which can result are shown in Figs. 2 and 3. In these examples, shear cracks have propagated from longitudinal and transverse defects or stress concentrations. In the case of Fig. 2, cracks have propagated on both the longitudinal and transverse shear planes to produce the typical star fracture found on surface hardened splined shafts when these are broken in torsional fatigue.

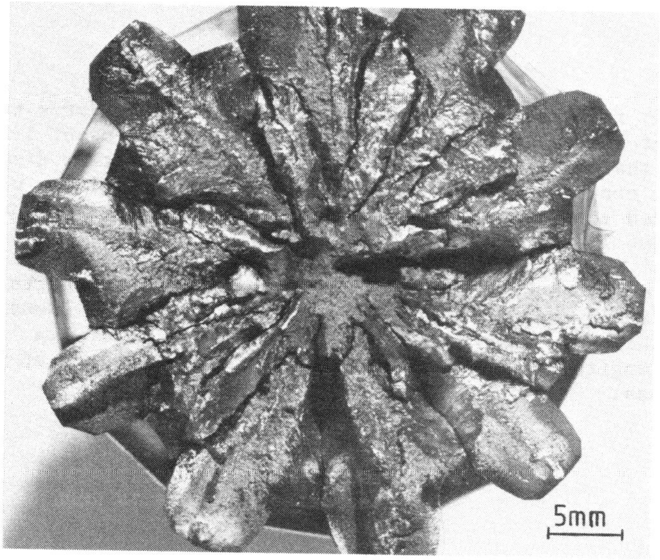

Fig. 2 Service failure of case carburised splined shaft showing longitudinal shear cracks emerging on transverse shear fracture face.

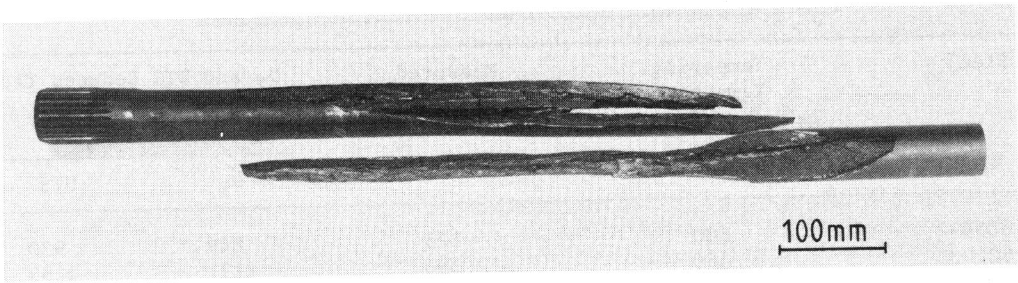

Fig. 3 Service failure of induction hardened shaft by propagation of longitudinal shear cracks.

Clearly, if critical defect sizes are to be assessed in such cases, then the shear modes of fracture are of primary interest. The limited experimental data which are available (Shah, 1974; Wilson, 1968) suggests that there is little correlation between K_{IC} and K_{IIIC} (that is, the critical stress intensities under modes I and III respectively), and hence the mode III toughness must be measured directly.

The stress state at the crack tip in mode III has been extensively analysed (e.g. Paris & Sih, 1965) and found to be biaxial. There will thus be far less constraint than in the plane strain mode I case, and flow stresses will be reduced.

In addition, the strength level in shear is approximately half that in uniaxial tension. Consequently the plastic zone in mode III is about 12 times that of the mode I equivalent, and use of an elastic-plastic fracture criterion for realistic specimen sizes and material strength levels is essential.

In this investigation, mode III data have been determined for two quenched and tempered steels using an approach analogous to the crack opening displacement in mode I. The results obtained are compared to those for mode I, and the micromechanisms are compared. Factors influencing the relative stabilities of the two modes in torsionally loaded components are examined.

EXPERIMENTAL DETAILS

Two quenched and tempered low alloy steels BS970 605H32 and 708H42 were selected for the initial investigation. These materials are commonly used for half-shafts and axles, and, by varying the tempering temperature, strength levels typical of the case and core of these induction hardened components could be obtained. A steel of intermediate strength level was also tested. The chemical composition, heat treatments, and mechanical properties are summarised in Tables I and II.

TABLE I Chemical Analysis (wt%)

Steel	C	Si	Mn	P	S	Cr	Mo	Ni	Al	Cu
605H32	0.33	0.20	1.55	0.017	0.029	0.32	0.23	0.35	0.03	0.28
708H40	0.41	0.27	0.69	0.032	0.022	0.99	0.25	0.23	0.03	0.29

TABLE II Mechanical Properties and Heat Treatment

Steel	Tempering Temperature ^oC	Measured Hardness HV30	σ_y and UTS deduced from Woolman and Mottram (MPa)	
			σ_y	UTS
605H32	600	325	849	930
605H32	450	390	1117	1283
605H32	300	540	1309	1463
708H42	575	400	988	1078
708H42	630	320	821	924

Conventional mode I fracture toughness data was obtained on 25mm thick compact tension specimens. The specimens were precracked to $a/w > 0.6$ according to the standard procedures (BS 5447 and Clarke and others (1979)). Plots of load against load-point-displacement were obtained by mounting a clip gauge across the loading pins. The toughness tests were conducted in displacement control. Values of the J integral were obtained at points of interest (viz crack initiation, maximum load and instability) by use of the expression developed by Merkle and Corten (1974). The corresponding values of the stress intensity factor K were obtained by using the relation

$$K_I = \left[\frac{EJ_I}{(1 - v^2)}\right]^{\frac{1}{2}} \qquad (1)$$

The initiation of slow, stable, crack growth was detected directly using a dc potential drop technique sensitive to ~0.05mm.

Circumferentially notched round bars of 25mm diameter were employed for the mode III fracture toughness testing. The bars were subjected to torsional loading in a closed-loop servo-hydraulic test machine with floating grips to eliminate any tensile forces. The specimens were fatigue precracked in torsion to a crack length (a) to radius (r) ratio of approximately 0.33. Cyclic torques of 350 Nm $\pm$ 300 Nm were found to be adequate for precracking, and the growth of the fatigue precrack was monitored using a dc potential drop technique sensitive to ~0.1mm.

During the toughness test the applied torque was plotted against the displacement of a clip gauge mounted across the notch so as to record the relative angular displacement of the crack faces. The tests were conducted under angular displacement control.

Values of the nominal stress intensity could be calculated using the expression from Rooke & Cartwright (1976)

$$K_{III} = f\left[\frac{a}{r}\right] \frac{2T}{r^3} \sqrt{\frac{a}{\pi}} \qquad (2)$$

where a is the crack length
r is the radius of the bar
T is the applied torque
and values of f(a/r) are given

However, it was found that for all the mode III tests, appreciable crack tip plasticity occurred, and use of the LEFM equation was inappropriate. Instead, an elastic-plastic approach was used, based on the crack sliding displacement (S), the mode III analogue of the crack opening displacement in mode I, McClintock & Irwin (1965); Knott (1973). At a given point of interest on the torque-clip gauge displacement curve, the sliding displacement could be obtained from the clip gauge displacement (C) by assuming that rotation occurs about the centre of the bar. Then, by a simple geometrical argument

$$\frac{S}{C} = \frac{r - a}{r + z} \tag{3}$$

where z is the height of the knife edges.

Values of K_{III} equivalent to a given sliding displacement could be obtained, in the spirit of the approach employed in mode I, by combining the equations (2, 3, 12)

$$G_{III} = \frac{\pi}{4} \tau_y S \tag{4}$$

and

$$G_{III} = \frac{K_{III}^2}{2\mu} \tag{5}$$

where μ is the shear modulus and τ_y is the yield stress in shear, assumed to be one-half the tensile yield stress. Values of the elastic constants are given by Woolman and Mottram (1964).

Since slow, stable crack extension occurred, a resistance curve could be generated for a single strength level in a manner analogous to that employed in mode I. A heat tint technique was employed to determine the amount of slow crack growth which had occurred. Specimens were heated for three hours at 300°C in a muffle furnace and were then broken apart by mode I fatigue in order to prevent any further smearing of the heat-tinted fracture surface. The amount of slow crack growth Δa was taken as the average of sixteen values taken around the circumference.

The dc potential drop technique was also used during the mode III toughness tests to detect crack initiation. The behaviour encountered was unusual in that the potential, which was constant during the initial stages of loading, fell to a minimum before rising steeply. The initial deviation was found to correspond to the onset of crack growth on the basis of the heat tint results. No obvious explanation is apparent for this anomalous behaviour.

RESULTS

The results of the mode I toughness tests are summarised in Fig. 4. For all strength levels other than the highest, no instability occurred during the tests, and the fracture mode was dimpled rupture. For the 605H32 tempered at 300°C, instability occurred at maximum load. In this case Scanning Electron Microscope (SEM) observations showed that the fracture mode was intergranular, which was not unexpected in a steel tempered in the 300°C tempered martensite embrittlement range. Figure 4 shows that the mode I initiation toughness falls as the strength level and hardness increase, in agreement with previous observations on quenched and tempered steels, Irving, Seah, Kurzfield (1976). The actual values obtained, varying between 50 and 130 $MNm^{-3/2}$ are similar to other low alloy steels heat treated to those strength levels.

The results of the mode III testing are summarised in Fig. 5. Values of K deduced from the crack sliding displacement approach were evaluated at initiation (K_{IIIi}), maximum torque (K_{IIIm}) and instability (K_{IIIc}). Fracture occurred by shear in all but the highest strength level material examined, and this resulted in a macroscopically flat fracture face, perpendicular to the axis of the bar. The macroscopic appearance of the fracture surface of a specimen of 605H32 tempered at 600°C is shown in Fig. 6, this appearance being typical. Flat facets (e.g. at A) form at the tip of the fatigue precrack (B). The facets are inclined to the plane of the precrack and they have the "factory roof" appearance observed by Pineau (1979) for facets formed under a combination of a static mode III load superimposed on a cyclic mode I. The facets developed by slow, stable, crack growth as is illustrated in Figure 7, which shows a specimen which has been heat tinted after interrupting the test. Areas of slow crack growth emanating from the fatigue precrack can be seen. Observations by scanning electron microscopy show that the facets are heavily smeared, and little information regarding the micromechanisms is readily available. However, closer inspection shows that elongated dimples may be observed in isolated regions (Fig. 8).

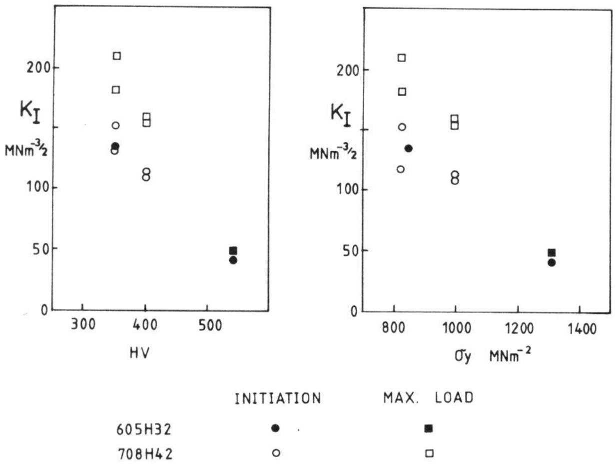

Fig. 4

Relation between mode I toughness and steel strength level and hardness

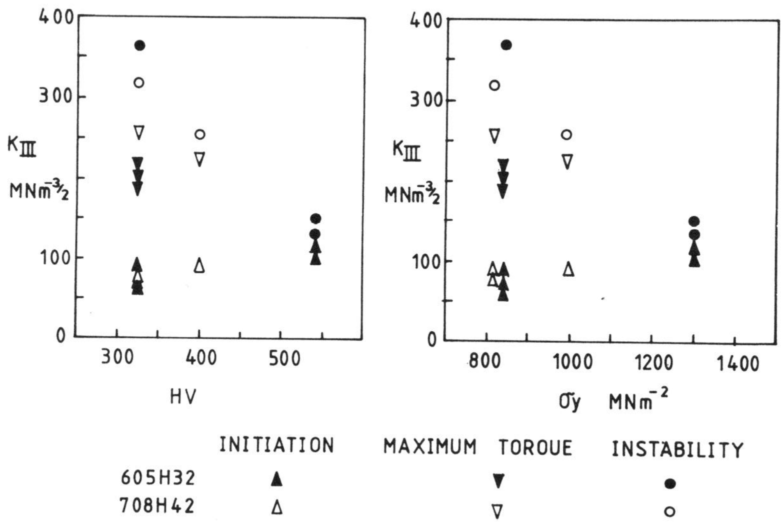

Fig. 5

Relation between mode III toughness and steel strength level.

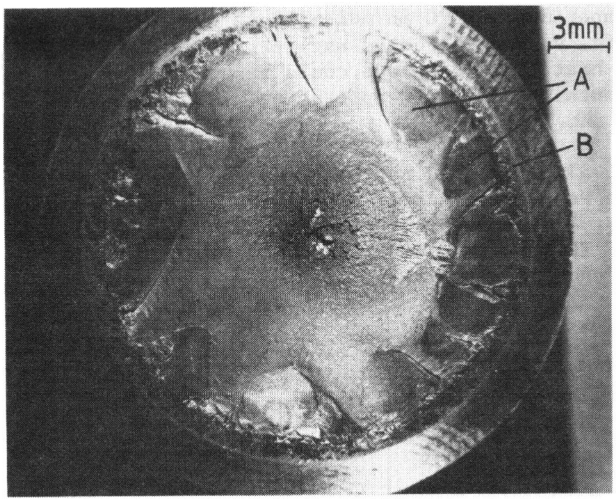

Fig. 6

Transverse shear fracture face of 605H32 steel tempered at 600°C and showing facets.

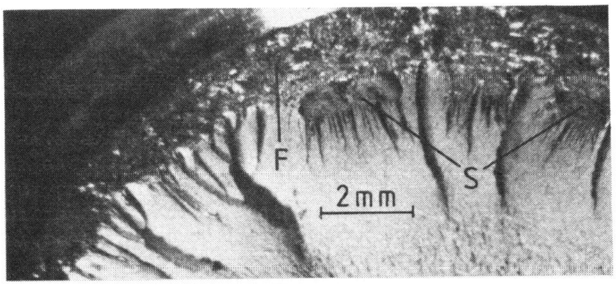

Fig. 7

Transverse fracture in 605H32 steel, showing Mode III fatigue precrack at F heat tinted slow crack growth region at S, followed by mode I fatigue cracking.

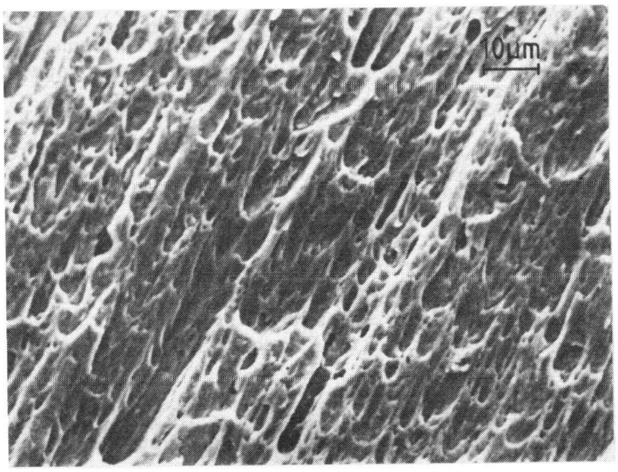

Fig. 8

SEM picture of void coalescence formed during mode III fracture.

The resistance curve for 605H32 tempered at 600°C in mode III as generated by the heat tint technique, is shown in Fig. 9. As discussed earlier, the start of slow crack growth as established by the heat tint technique could be correlated with the initial deviation in DC potential output. This interpretation was thus used in all tests.

The large degree of scatter in the values deduced by the PD method is due to a certain extent to the steepness of the resistance curve. The curve for 605H32 tempered at 600°C, has the value of S (or K_{III}) at instability considerably greater than the corresponding value at initiation. This is predicted for ductile materials by the theoretical analysis of McClintock and Irwin (1965).

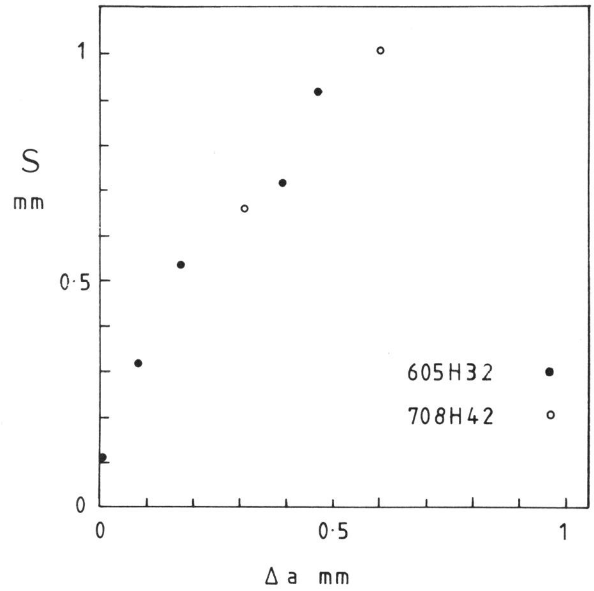

Fig. 9

Relation between crack sliding displacement S and crack advance Δa.

In contrast to the behaviour exhibited at lower strengths, the highest strength material investigated (605H32 temp. at 300°C) fractured with a considerable component of mode I, resulting in a fracture plane perpendicular to the maximum tensile stress. The fracture behaviour in this case is clearly dominated by mode I cracking and the fracture mode is a mixture of intergranular and dimpled rupture, although it is not clear from the fractographic observations whether or not any initial extension by mode III is necessary to produce a suitably oriented microcrack which then propagates under the action of the tensile stress.

DISCUSSION

Figure 4 illustrates that the mode I fracture toughness of these steels, whether corresponding to maximum load or initiation, decreases with increasing strength level. In the case of the highest strength steel, part of this decrease is attributable to a change of fracture mode from dimpled rupture to that of intergranular. However, mode I toughness tests on steels of varying strength level, and which retain the dimpled rupture fracture mode up to yield strengths of 1500 - 1600 MPa (Irving, Seah and Kurzfeld, 1976) show that the mode I toughness still decreases with increasing strength level.

In contrast to this trend, the resistance to crack initiation in mode III (Fig. 5) increases with strength level. Again, it is to be noted that the highest strength material had a substantial component of intergranular fracture present, but the initiation toughness figure obtained can be regarded as a minimum, as mode I cracking intervened. It may be stated that the mode III initiation toughness value is at least as great as that value which was measured; it may well be higher still, confirming the unusual trend of increasing resistance to the onset of slow, stable, crack growth with increasing strength. Although the values of K_{III} at initiation increase, the values of K_{III} at instability decrease with increasing strength, with the behaviour of the highest strength material being dominated by cracking under tensile stresses. The fact that the instability values decrease, while the initiation ones increase, illustrate the general point that the resistance to initiation and the resistance to slow, stable, cracking may vary independently (Willoughby, Pratt, Turner, 1978).

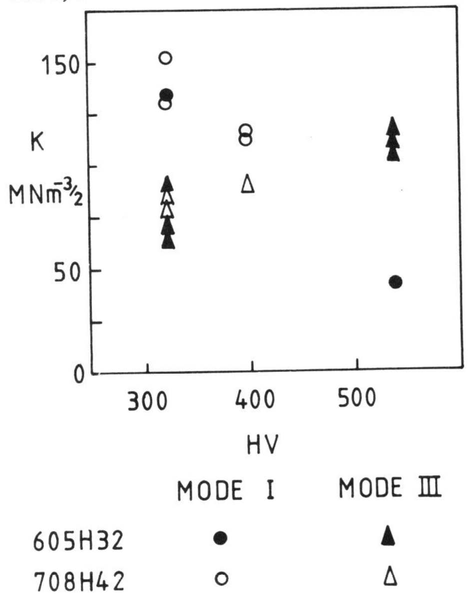

Fig. 10

Comparison of mode I and III initiation toughness values.

The very different initiation behaviour of the two modes when the strength level is varied (Fig. 10) may be attributed to differences in the crack tip stress state. The decrease in the mode I toughness with increasing strength level is due to the influence of a number of factors, as follows. Increasing the yield stress results in an increase in the triaxial stress field at the crack tip, and this increased triaxiality results in a reduction of the local strain to fracture (Hancock, Cowling, 1980), and hence the fracture toughness. Another factor of importance is the work hardening capacity, which decreases with increasing yield strength, this decrease ultimately resulting in the occurrence of "fast shear" rather than microvoid coalescence (Knott, 1980), with a further decrease in toughness. A further effect is that the particles controlling the void nucleation and coalescence process may be different for different heat treatments (Gerberich, 1979). As a result, simple models, based on such parameters as fracture strain, yield strength, strain hardening exponent, and, in some cases, a size parameter, may fail to predict the observed decline in toughness with increasing strength level in quenched and tempered steels. This has recently been summarised by Gerberich (1979). In contrast to the mode I case, the mode III configuration is a biaxial one, and hence the local strain to fracture at the crack tip will only be influenced by the material properties directly, without the additional effect of the variation of triaxiality with yield strength. If the effects of strength level and work hardening rate alone on toughness are similar in the two modes then removal of triaxiality will have the effect of increasing ductility to fracture at the higher strength levels, and toughness will increase compared with the mode I case. Thus it is to be expected that the trend of decreased toughness with increased strength level will be less pronounced in mode III and may even be reversed. The fact that a reversed trend is observed, perhaps provides an indication of the relative importance of the triaxial stress field in reducing ductility to fracture.

Since K_{IIIi} is slightly lower than K_{Ii} at the lower strength level, growth of the crack under mode III loadings by a "true" mode III mechanism is expected. On the other hand, for the 605H32 steel tempered at 300°C, K_{Ii} is considerably less than K_{IIIi}, and the material would be expected to be prone to mode I cracking, as is the case. In the absence of compressive residual stresses the fracture behaviour of this material is dominated by the resistance to mode I cracking (at least for the stages in the fracture process subsequent to the production of a "mode I" microcrack from the fatigue precrack) rather than that to mode III cracking. Hence, as the strength level increases, K_{Ii} decreases relative to K_{IIIi}, and the material becomes increasingly prone to failure under the action of tensile stresses rather than the true shear mode. The results therefore provide a rationale for the fracture behaviour in service of high and low strength level materials when these are broken in torsion.

ACKNOWLEDGEMENTS

Thanks are due to V. Kumar for assistance with the experimental work, and M. S. Starkey for helpful discussions. The paper is published by permission of Dr. T. L. Johnston, Director, GKN Technology Ltd.

REFERENCES

British Standard No. 5447 (1977), Method of test for plane strain fracture toughness (K_{IC}) of metallic materials.

Clarke, G. A., Andrews, W. R., Bagley, J. A., Ronald, J. K., Embley, G. T., Landes, J. D., McCabe, D. E. and Underwood, J. H. (1979). A procedure for the determination of ductile fracture toughness values using J integral techniques. J. Testing & Eval., Vol. 7, 49 - 56.

Dieter, G. E. (1961). Mechanical Metallurgy. McGraw-Hill, New York.

Gerberich, W. W., Stant, M., Jatavallabhula, K. and Atteridge, D. (1979). Acoustic emission interpretation of ductile fracture processes. Int. J. Frac. 15. 491 - 514.

Hancock, J. W. and Cowling, M. J. (1980). The role of state of stress on crack tip failure processes. Conference on Micromechanisms of Crack Extension, Cambridge.

Hourlier, F. and Pineau, A. (1979). Fatigue cracking under complete stress of a rotor steel. Mem. Sci. Rev. Met. 175 - 185.

Irving, P. E., Seah, M. P. and Kurzfeld, A. (1976). Proceedings of the Second International Conference on Mechanical Behaviour of Materials, Boston. 563 - 567.

Knott, J. F. (1973). Fundamentals of fracture mechanics. Butterworths, London.

Knott, J. F. (1980). Micromechanisms of crack extension in engineering alloys. Conference on micromechanisms and crack extension. Cambridge.

McClintock, F. A. and Irwin, G. R. (1965). ASTM STP 381. 84 - 113.

Merkle, J. G. and Corten, H. T, (1974). A J integral analysis for the compact specimen considering axial as well as bending effects. ASME paper No. 74 - PVP - 33.

Paris, P. C. (1977). Fracture mechanics in the elastic-plastic regime, ASTM STP 631. 1 - 26.

Paris, P. C. and Sih, G. C. (1965). Stress analysis of cracks. ASTM STP 381. 30 - 81.

Rice, J.R. (1968). In H. Liebowitz (Ed.) Fracture Vol. 2. Academic Press, London. Chap. 3. 191 - 311.
Rooke, D. P. and Cartwright, D. J. (1976). Compendium of stress intensity factors. HMSO, London.
Shah, R. A. (1974). Fracture under combined modes in 4340 steel. ASTM STP 560. 29 - 51.
Smith, R. A. (1980). Mechanisms of mode II (sliding) crack advance. Session 5J, Conference on Micromechanisms of Crack Extension, Cambridge.
Sorensen, E. P. (1978). A finite element investigation of crack growth in antiplane shear. Int. J. Frac. 14. 485 - 500.
Willoughby, A. A., Pratt, P. L. and Turner, C. E. (1978). The effect of specimen orientation on the R-curve. Int. J. Frac. 14. R249 - R251.
Wilson, W. K., Clark, W. G. and Wessel, E. T. (1968). Fracture Mechanics Technology for combined loading and low to intermediate strength metals. Final Technical Report No. 10276, Westinghouse Research Laboratories.
Woolman, J. and Mottram, R. A. (1964). The mechanical and physical properties of the British Standard EN steels. Macmillan, New York.